Journal of Engineering Mathematics **49:** 77–97, 2004.

Inertia effect on a structure of pressure-driven flames in porous media

VIATCHESLAV BYKOV, IGOR GOLDFARB and VLADIMIR GOL'DSHTEIN
Ben-Gurion University of the Negev, Department of Mathematics P.O.B.653, Beer-Sheva 84105, Israel
vbykov@cs.bgu.ac.il; goldfarb@cs.bgu.ac.il; vladimir@bgumail.bgu.ac.il

Received 13 November 2002; accepted in revised form 21 August 2003

Abstract. The phenomenon of a subsonic pressure-driven flame in an inert porous medium filled with a flammable gaseous mixture is considered in the present work. The paper focuses on the analysis of the impact of the inertia of a fluid on the fine structure of the flame front and its velocity. In the frame of reference attached to an advancing combustion wave and after a suitable non-dimensionalization the corresponding mathematical model includes three highly nonlinear ordinary differential equations (ODEs). The system is converted into a singularly perturbed system of ODEs by a suitable choice of new phase coordinates and then treated analytically along the lines of a suggested asymptotic machinery (modified version of the method of invariant (integral) manifolds - MIM). According to the MIM, an arbitrary solution of the initial system of ODEs under consideration is represented as a trajectory in the phase space. It is shown that two principally different parts of the trajectory exist: fast motion from the initial point to a slow curve and another fast motion from the matching point lying on the slow curve to the singular (final) point of the system. The first stage is associated with a pre-heat subzone of the flame, whereas the second is interpreted as a reaction subzone. It is demonstrated that the matching point of these two parts of the trajectory plays a crucial role in the description of the flame characteristics. The proposed analytical approach allows one to obtain an analytical expression for the effect of inertia on the flame velocity. The theoretical predictions show reasonably good agreement with data resulting from direct numerical simulations.

Key words: inertia of gas mixture, integral manifolds, porous media, pressure-driven flames, slow curve

1. Introduction

Recently, there has been a surge of interest in the combustion of gaseous mixtures within porous inert media [1–4]. Flames stabilized within the porous matrix have higher burning speeds and distinct flammability limits than open flames. There are a number of possible explanations of the phenomenon, namely: internal feedback of heat from the burned to the unburned gases through radiative heat transfer, conventional heat conduction through a solid skeleton, diffusion of a heated gas due to a local pressure elevation, etc. We will focus on the latter: a local pressure elevation.

The conventional approach to flame-propagation modelling in open air ignores pressure perturbations. This is reasonable because the flame-propagation velocity in open air is significantly lower than the speed of sound. This assumption is well founded in a number of combustion problems considered in the literature. It means that pressure disturbances move away from the reaction zone so fast that their influence on the intensity of the thermal processes is negligibly small.

This conclusion is not correct for gaseous combustion processes in inert porous media, because (for comparatively narrow pores) the speed of a pressure perturbation may be significantly lower than the sound velocity, in open air. Under such circumstances a local elevation

of the pressure may lead to the formation of a self-sustaining combustion wave controlled by pressure diffusion.

In recent papers [2–4] this heuristic idea has been converted into original models that describe a new physical mechanism of flames spreading through inert porous media. The model assumes that, in compartively narrow pores, the propagation of combustion waves may be governed mainly by diffusion of pressure (so-called barodiffusion) in porous media, rather than by conventional heat transfer (thermal diffusion). Using the δ-function approximation of the reaction zone (high-activation-energy assumption), the authors of [2] demonstrated that the flame velocity in a porous medium may be sufficiently higher than in open space (caused by conventional thermal-conductivity thermodiffusion). Later the existence of a travelling-wave solution was proved in [3, 4] under the additional simplifying assumption of weak heat release. The transition from low-velocity regimes (governed by conventional thermal conductivity) to high-velocity regimes (controlled by pressure diffusion) was analyzed.

Traditionally the study of premixed gas flames in open space makes use of asymptotic techniques. In particular, the method of inner and outer expansions represents a powerful and effective tool for analyzing the structure and the velocity of flames in various media. Unlike conventional deflagration, in pressure-driven flames, the temperature within the reaction zone undergoes a nearly jumpwise increase, whereas the preheat zone is rather wide and the temperature growth within it relatively slow. As a result the traditional multiple-scale approach developed for tackling deflagrations analytically meets with formidable difficulties. The present work aims to overcome this hurdle and evaluate the main characteristics of the propagating flame. In this paper we demonstrate how the powerful method of integral manifolds (MIM) [5], [6, Chapter 2], [7, Chapter 1], [8]] can be successfully applied to this relatively new field, namely the problem of pressure-driven flame propagation through a two-phase medium (inert solid skeleton filled with a flammable gaseous mixture).

The goal of the present paper is to study the impact of the inertia of the gaseous mixture on flame propagation and to elucidate the effect of the inertia on the fine structure and main characteristics of the flame front. The derived analytical formulas show reasonably good agreement with results obtained by relevant numerical simulations.

2. Problem statement

We will use a model developed in [9–11]. The conventional single-temperature approach and cell model are incorporated into the model. We restrict ourselves to a one-dimensional approach, assuming that it gives us conceptual qualitative information about the main dynamical properties of the process. The porous medium is considered as a set of evenly spread parallel capillaries of the same inner radius (so-called cell model), filled with a premixed combustible gas mixture (the solid matrix is inert). The presence of the porous medium is accounted for by the friction force (velocity-dependent) added to the momentum equation. The combination of the inner capillary radius and gas-mixture viscosity may lead to the appearance of so-called creeping flow of the reactant mixture. This flow regime corresponds to a low Reynolds number Re. As in [9, 10] we assume that the friction force is internal, and does not affect the total energy balance of the system.

To single out the pure impact of the pressure effect on the properties of a self-sustained combustion wave driven by a local pressure elevation, the conventional mechanism of combustion-wave propagation (thermal diffusion) is regarded as negligibly small (compared with

pressure diffusion, *i.e.* barodiffusion) and it is thus excluded from our consideration. Additionally, this allows us to simplify the mathematical description of the actual extremely complex problem and to make it tractable analytically. Presumably, the approximated problem preserves most of the basic features of the originally full nonlinear system.

Within the above constraints, the system of governing equations contains energy (1), concentration (2), momentum (3), continuity (4), state (5) equations, and reads

$$\frac{\mathrm{d}}{\mathrm{dx}}\left(\rho(u-D)(c_v T+\frac{1}{2}u^2)+Pu\right)=QW, \tag{1}$$

$$\frac{\mathrm{d}}{\mathrm{dx}}(\rho(u-D)C_f)=-W, \tag{2}$$

$$\frac{\mathrm{d}}{\mathrm{dx}}\left(\rho(u-D)u+P\right)=-K_F\rho u|u|, \tag{3}$$

$$\frac{\mathrm{d}}{\mathrm{dx}}\left(\rho(u-D)\right)=0, \tag{4}$$

$$P=\frac{\rho}{\mu}RT=(c_p-c_v)\rho T. \tag{5}$$

Here a friction force (RHS of Equation (3)) is taken proportional to the square of the local gas velocity u, which corresponds to the Forcheimer equation [11], and the reaction rate W is taken in the conventional form of an Arrhenius law for a one-step reaction of the first order:

$$W=AC_f\,\rho\exp(-E/RT). \tag{6}$$

The following notations have been used: T – temperature (K); P – pressure (Pa); E – activation energy (J/kmol); D – velocity of the flame front in the laboratory system of coordinates (m/s); C – concentration of the deficient reactant; c – specific heat capacity (J/kg/K); u – gas velocity in the laboratory frame of reference (m/s); Q – combustion energy (J/kg); W – reaction rate (kg/(s m^3)); ρ – density (kg/m^3); K – permeability of the medium (m^2); ν – kinematical viscosity (m^2/s); A – pre-exponential (frequency) factor (1/s); R – universal gas constant. Subscripts mean: f – combustible component of the gas mixture; p – under constant pressure; v – under constant volume; 0 – undisturbed state; b – burnt (behind the combustion wave front), F – related to the case of quadratic dependence of the friction force on gas velocity. The system (1–5) is subject to boundary conditions (fresh mixture far ahead of the front of the flame)

$$T(x\to+\infty)=T_0,\ C_f(x\to+\infty)=C_{f0},\ P(x\to+\infty)=P_0,\ \rho(x\to+\infty)=\rho_0. \tag{7}$$

The system (1–6), together with the boundary conditions (7), represents a complete mathematical description of the problem under consideration.

2.1. Dimensionless system

To simplify the analysis further, let us introduce dimensionless variables along the lines of the Semenov approach, which is well-accepted in thermal-explosion theory [12], [13, Chapter 2]. These dimensionless variables are defined as follows:

$$\xi=-\frac{x}{D}A\exp\left(-\frac{1}{2\beta}\right),\quad \beta=\frac{RT_0}{E}, \tag{8}$$

$$\eta = \frac{C_f}{C_{f0}}, \quad \theta = \frac{1}{\beta}\cdot\frac{T-T_0}{T_0}, \quad \Pi = \frac{1}{\beta}\cdot\frac{P-P_0}{P_0}, \tag{9}$$

where Π is the dimensionless pressure; θ the dimensionless temperature; η the dimensionless concentration of deficient reaction and ξ the automodel variable (dimensionless).

One of the main advantages of the proposed dimensionless variables is their independence of the final temperature and pressure of the reaction products (mixture parameters behind flame front). The dimensionless variables (9) are introduced with respect to the initial values of the corresponding dimensional ones. This gives us an opportunity to consider the final temperature and pressure as unknown parameters, which are to be found. Additionally, it allows us to rewrite the originally multi-scale system (due to the presence of processes with essentially different characteristic times) in the conventional form of a singularly perturbed system of ordinary differential equations that allows us in turn to apply appropriate asymptotic methods.

Making use of the expressions (8–9), one may rewrite the original system of equations in the form

$$\frac{d\theta}{d\xi} = \frac{\left(1-\varepsilon_{\text{inert}}\frac{(\Pi-\theta)(1+\beta\theta)}{(1+\beta\Pi)^3\sigma}\right)H_F(\theta,\Pi)+\left(1-\varepsilon_{\text{inert}}\frac{1+\beta\theta}{(1+\beta\Pi)^2\beta\sigma}\right)H_R(\theta,\Pi,\eta)}{\left(1-\varepsilon_{\text{inert}}\frac{(1+\beta\theta)}{(1+\beta\Pi)^2\beta\sigma\gamma}\right)}, \tag{10}$$

$$\sigma\frac{d\Pi}{d\xi} = \frac{\left(1-\varepsilon_{\text{inert}}\frac{(\Pi-\theta)}{(1+\beta\Pi)^2}\right)H_F(\theta,\Pi)-\frac{\varepsilon_{\text{inert}}}{(1+\beta\Pi)\beta}H_R(\theta,\Pi,\eta)}{\left(1-\varepsilon_{\text{inert}}\frac{(1+\beta\theta)}{(1+\beta\Pi)^2\beta\sigma\gamma}\right)}, \tag{11}$$

$$\frac{d\eta}{d\xi} = -\varepsilon_2\eta\frac{1+\beta\Pi}{1+\beta\theta}\exp\left(\frac{\theta}{1+\beta\theta}\right), \tag{12}$$

$$H_F(\theta,\Pi) = \lambda_{\text{F}}^3\frac{(\Pi-\theta)|\Pi-\theta|}{(1+\beta\theta)(1+\beta\Pi)}, \quad H_R(\theta,\Pi,\eta) = \varepsilon_1\eta\frac{1+\beta\Pi}{1+\beta\theta}\exp\left(\frac{\theta}{1+\beta\theta}\right), \tag{13}$$

where the following dimensionless parameters are given by

$$\varepsilon_1 = \frac{C_{f0}Q}{c_pT_0\beta}\exp\left(-\frac{1}{2\beta}\right), \quad \varepsilon_2 = \exp\left(-\frac{1}{2\beta}\right), \ \varepsilon_1 \ll 1, \ \varepsilon_2 \ll 1, \tag{14}$$

$$\varepsilon_{\text{inert}} = \frac{\beta D^2}{c_pT_0} \ll 1, \quad \sigma = 1-\frac{1}{\gamma}, \quad \gamma = \frac{c_p}{c_v}$$

and the dimensionless flame speed λ_F is defined in the following way (subscript F denotes the quadratic dependence of the friction force on the local gas velocity)

$$\lambda_F^3 = K_F\frac{\beta D^3}{c_pT_0A}\exp\left(\frac{1}{2\beta}\right). \tag{15}$$

Let us remark also that the straight line $\Pi = \theta$, $\eta = 0$ is a line of singular points of the system (10–12). Note also, that the problem under consideration contains the unknown parameter (dimensional flame velocity D) as a part of the two distinct dimensionless combinations ($\varepsilon_{\text{inert}}$,

responsible for the impact of the inertia of the gaseous mixture, and λ_F, dimensionless flame velocity). This feature defines the main extent of the high level of complexity of the formulated problem.

2.2. Energy integral and reduced system

The system (10–12) is adiabatic; therefore the energy integral exists and can be easily derived. It reads

$$\eta - 1 + \frac{\varepsilon_2}{\varepsilon_1}(\theta - \sigma\Pi + \frac{1}{2}\varepsilon_{\text{inert}}\frac{(\Pi - \theta)^2}{(1 + \beta\Pi)^2}) = 0. \tag{16}$$

Additionally, the system (10–12) permits us to conclude that the unique singular point of the system is characterized by an equality of the dimensionless temperature θ_b and pressure Π_b. This point corresponds to the final point of the phase trajectory representing the flame front in (Π, θ, η) – phase space. Assuming that the reaction has been completed in the region of a burnt mixture (*i.e.*, $\eta_b = 0$) and using the energy integral (16), one can deduce that the coordinates of the final point (main characteristics of the medium behind the flame front) are as follows

$$\theta_b = \Pi_b = \frac{\varepsilon_1}{\varepsilon_2(1 - \sigma)} = \frac{\varepsilon_1\gamma}{\varepsilon_2},\ \eta_b = 0. \tag{17}$$

The presence of the energy integral (16) allows us to exclude one of the variables (say, the dimensionless concentration η), thus reducing the number of independent equations by one. The energy integral (16) provides us with the expression $\eta = \eta(\theta, \Pi)$, which can be substituted in the equations for the temperature (10) and pressure (11). The reduced system contains the two ODEs (10–11) where the functiosn H_R and H_F and $\eta = \eta(\theta, \Pi)$ are given by relations (13) and (16), respectively.

It is clear that a qualitative analysis of the reduced system (10–11), using standard methods, is made extremely difficult by the complexity of the right-hand sides of the equations. Therefore, appropriate numerical procedures must be resorted to. Alternatively, the presence of the sufficiently different time scales raises the possibility of using some kind of asymptotic procedure. In this paper, we exploit a powerful technique, namely a geometrical version of the integral (invariant) method (MIM), which permits us to decompose a phase-space analysis of an arbitrary multi-scale system into separate studies of its fast and slow subsystems. This decomposition can be different for different flame zones. The advantage of this decomposition is that any subsystem has lower dimensions than the original one. Results of this geometrical/analytical study usually have a compact, clear rendition in terms of the physicochemical parameters of the system. Although numerical solution of the Equations (10–11) is straightforward, a general analytical parametric analysis of the system behaviour, such as will be presented here, is unattainable by numerical means.

3. Analysis and results

3.1. MIM – SHORT DESCRIPTION

Before proceeding with the analysis, we diverge to give a brief general description of this approach. The essence of any qualitative study of a multi-scale system involves analyses of the processes sequentially, moving from the fastest to the slowest. Consider an arbitrary multi-scale hierarchical system. Suppose that a particular process is associated with a certain scale. Then, to leading order, all slower processes will be 'frozen', whereas all faster processes will have reached a 'quasistationary' state (in the sense that their rate of change will have already approached that of the given particular process). Note that, in a general case, the 'quasi-stationary' state can be temporary, with the process becoming fast again in a finite period of time.

Now consider an arbitrary parametric region where there exists a clear distinction between the rates of change of the various variables. Suppose that a single variable is fastest and all the other variables can be considered as slowly varying with the same rate of change. Asymptotically, the rate of change of the fastest variable is infinitely greater than that of the other variables. Let us choose an initial point in the space of variables under consideration and contrast further development of their dynamical behavior. Upon comparing the relative change of the variables, we conclude that, while the value of the fastest one varies, all others will conserve their initial values (because their rates are infinitely less than that of the fastest variable). This situation is maintained until the moment when the fastest variable approaches its 'steady state'. The latter is the point at which the rate of change of the fastest variable becomes of the same order of magnitude as the rates of change of the other variables. At this point another stage of the dynamical process begins (the slow part), which is characterized by some type of balance between the rates of change. Mathematically this balance represents a functional relation determining a hyper-surface (slow invariant manifold). The lower dimension (by one) of the hyper-surface, where the slow stage begins, is analytically advantageous. Also, in turn, the slow stage can once again be subdivided into fast and slow regions and the entire analysis can be repeated. The relevant mathematical background of this sort of analysis can be found in the theory of integral (invariant) manifolds [5], [6, Chapter 2], [7, Chapter 1], [8, 14]. An original version of the integral manifolds method [6, Chapter 2] was adapted for combustion problems in [8]. The technique of MIM has proved to be highly successful in unraveling problems of gaseous combustion, including flame propagation in porous media [10, 15, 16].

3.2. SINGULARLY PERTURBED SYSTEM

To successfully perform an asymptotic analysis of the system (10–11), it would make sense to divide the flame front into two subzones along the lines of Zel'dovich's approach [17, Chapter 4]. The subdivision into two qualitatively different subzones, which are usually referred to as the preheat and the reaction zones, is possible due to the nature of the Arrhenius reaction term and the assumption of high activation energy. In turn, the existence of the two subzones leads to a similar subdivision of the physically interesting region of the phase plane into two corresponding sub-regions. The problem considered here may be reformulated and solved within each of the two subregions on the basis of its specific properties. The asymptotic solutions obtained separately in these subregions are then to be matched. To reach the

aforementioned aim, it would be worthwhile to reformulate the original problem in a form treatable by the suggested approach.

Despite a sufficient difference in characteristic times of the processes involved, the system (10–12) and the reduced system (10–11) (note that the third variable, the concentration η, can be excluded from consideration due to the existence of the energy integral) are not directly treatable by the chosen asymptotic tool (MIM). The reason is that the pair of Equations (10–11) does not represent a singularly perturbed system of ODEs in a conventional form. To make the Equations (10–11) tractable for the MIM, we need to introduce a pair of new variables instead of the existing θ and Π. The new variables should allow us to emphasize the difference in time scales.

There are a number of basic principles that can be exploited to exchange the variables. The physical rationale lying behind the choice made in the present paper is rather simple. The key to the suggested approach lies in the suitable utilization of these features, which allows us to re-formulate the original problem as two separate sets of ODEs written in pure SPS form (treatable by the adopted asymptotic tool): the new variables are chosen as deviations from the corresponding approximate conservation laws.

It makes sense to follow the previous order of analysis: from preheat subzone to the reaction zone. Within the preheat subzone an input of the exothermic chemical reaction is assumed to be negligible, whereas the friction force plays a dominant role in the system dynamics. As a result, the system energy remains almost constant and we can interpret this fact as the existence of an approximate law of energy conservation in this subzone. On the other hand, the momentum of the system changes essentially within the preheat subzone. Hence, one of the new variables can be introduced as a deviation from the approximate law of energy conservation (in the absence of reaction)

$$v = \theta - \sigma\Pi + \frac{1}{2}\varepsilon_{\text{inert}}\frac{(\Pi - \theta)^2}{(1 + \beta\Pi)^2}. \tag{18}$$

Having determined a new variable v (18), a *slow* alteration of the introduced variable within the preheat subzone is expected.

Note here, that the preheat subzone (subzone of preliminary heating of the fresh mixture in the head of the flame) should be called the ‘pre-pressure’ zone, because thermal diffusion is excluded from consideration and heat is transferred due to pressure diffusion. Therefore, the term ‘preheat’ accepted in the paper is used conditionally to some extent.

All aforementioned arguments can be repeated *mutatis mutandis* for the reaction subzone. The preheat subzone is distinguished by a negligible chemical-reaction impact. Conversely, the reaction subzone is characterized by a dominant role of the heat release due to the chemical reaction. The influence of the other processes (hydraulic resistance) is assumed to be of minor importance. Therefore, unlike the preheat subzone, the reaction subzone can be typified by another approximate conservation law – the system momentum conservation. Similar to the introduced variable v (18), a second new variable u can be determined as a divergence from the approximate law of momentum conservation

$$u = \sigma\Pi - \frac{\varepsilon_{\text{inert}}}{\beta}\frac{\Pi - \theta}{1 + \beta\Pi}. \tag{19}$$

The right-hand side of expression (19) represents the dimensionless form of the momentum equation (3). A clear advantage of this definition is our expectation that the new variable u will be *slow* within the reaction subzone.

The introduced variables v and u permit us to rewrite system (10–11) in the following form

$$\frac{\mathrm{d}v}{\mathrm{d}\xi} = H_R(\theta(u, v), \Pi(u, v)), \tag{20}$$

$$\frac{\mathrm{d}u}{\mathrm{d}\xi} = H_F(\theta(u, v), \Pi(u, v)). \tag{21}$$

Remember that both of the introduced variables are expected to be slow in the *different* subzones: v (20) – within the preheat subzone, u – within the reaction subzone. To justify this conclusion and further analysis, let us compare the rates of changes of the variables v, u with each other in each of the two subzones.

In the preheat subzone the temperature of the mixture is close to the initial value (zero) and one can conclude that the Arrhenius exponent is of the order $O(1)$. Therefore, to leading order, the terms H_R and H_F, with respect to the small parameter β, are as follows

$$H_R \sim \frac{1}{\beta}\exp\left(-\frac{1}{2\beta}\right), \quad H_F \sim \beta\exp\left(\frac{1}{2\beta}\right). \tag{22}$$

The ratio of these two terms (H_R, H_F) determines the relation between the RHSs of Equations (20–21) and it reads

$$\frac{H_R}{H_F} \sim \frac{1}{\beta^2}\exp\left(-\frac{1}{\beta}\right) \ll 1. \tag{23}$$

The inequality (23) means, in particular, that within the preheat subzone the variable u is much faster than the variable v. The deduction made justifies our previous conclusion (v was expected to be slow within the preheat subzone).

Within the reaction subzone the situation differs from that in the preheat one. The temperature of the gaseous mixture comes close to the temperature of the burnt combustion products, which is determined by Equation (17). Therefore, one can suppose that the temperature θ is of the order $\varepsilon_1/\varepsilon_2$, which leads us to the conclusion that the Arrhenius term H_R is exponentially large within the reaction subzone, whereas the hydrodynamic term H_F remains the same

$$H_R \sim \varepsilon_1\exp\left(-\frac{\varepsilon_1/\varepsilon_2}{1+\beta\varepsilon_1/\varepsilon_2}\right) \sim \frac{1}{\beta}\exp\left(\frac{1}{2\beta}\right), \; H_F \sim \beta\exp\left(\frac{1}{2\beta}\right). \tag{24}$$

Expressions (24) allow us to derive a corresponding relation between the two RHSs of the Equations (20–21) in this subzone

$$\frac{H_R}{H_F} \sim \frac{\frac{1}{\beta}\exp\left(\frac{1}{2\beta}\right)}{\beta\exp\left(\frac{1}{2\beta}\right)} = \frac{1}{\beta^2} \gg 1. \tag{25}$$

The inequality (25) simply demonstrates the well-known fact that, within the thin subzone, where an exothermic chemical reaction takes place, the Arrhenius term H_R plays a leading role and it dominates the hydraulic resistance term H_F. Hence, the rate of change of the variable u is much *slower* than that of v within the reaction subzone. As in the previous case this justifies our preliminary conclusions based on the suggested way of choosing the variable u (u was expected to be slow within the reaction subzone).

To successfully perform an asymptotical analysis of the system (10–11) it will make sense to introduce one more auxiliary variable, which has the *same* rate of change within the two-subzones. To reach the declared aim, let us define a new variable w as the difference between the two former ones

$$w = u - v = 2\sigma\Pi - \theta - \frac{1}{2}\varepsilon_{\text{inert}}\frac{(\Pi-\theta)^2}{(1+\beta\Pi)^2} + \frac{\varepsilon_{\text{inert}}}{\beta}\frac{\Pi-\theta}{1+\beta\Pi}. \tag{26}$$

The new variable w has a distinguishing feature: it is a fast variable within both subzones. Indeed, a corresponding ODE determining the dynamics of the new variable w can be written in the form

$$\frac{\mathrm{d}w}{\mathrm{d}\xi} = H_R(\theta(w,v),\ \Pi(w,v)) - H_F(\theta(w,v),\ \Pi(w,v)), \tag{27}$$

To clarify the statement made above, one only needs to compare values of the RHSs of (20), (21), (27). In other words, we will compare the rates of change of the variables u, v, w in the distinct subzones of the flame front.

One can see that Equation (27) contains both terms H_R, H_F, whereas each of the Equations (20) and (21) includes only one of these two terms. As was shown earlier, within the preheat subzone, the term H_R is exponentially small with respect to H_F and the inequality (23) is valid. Therefore, the rate of change of the new variable w is determined by the hydraulic resistance term H_F and the variable w varies much faster than the variable v (note that the definition of the variable v causes it to alternate slowly within the preheat subzone). In a similar way we can deduce that, within the reaction subzone, where the Arrhenius term H_R is exponentially large with respect to H_F, and the inequality (25) is valid, the behaviour of the new variable w is determined by the reaction term H_R. Hence, the variable w transforms much faster than the variable u (note that, due to choice of the variable u, it changes slowly within the reaction subzone). To recap these estimates, we summarize that the variable w (26) is *fast* within *both* sub-zones.

The reasons mentioned above permit us to conclude that the current system of governing equations decouples into two different singularly perturbed systems of ODEs within the appropriate subzones of the flame front. Both systems contain one of the pair of Equations (20) or (21) and a differential Equation (27) for the new variable w.

Thus, there is a good reason to consider a flame configuration within the preheat subzone governed by the pair of Equations (20), (27) (v – slow, w – fast), whereas the combustion-wave structure within the reaction subzone will be better described by the pair (21), (27) (u – slow, w – fast). This decomposition permits us to rewrite the original system (10–11) as two separate systems for the different subzones of the flame. Each of these systems has the conventional form of a singularly perturbed system of ODEs making direct application of the MIM legitimate.

3.3. Flame-front structure – subzones

We now turn to the analysis of the possible dynamical scenarios of the solutions of the reduced system (10–11). We catalogue the different possibilities according to the criteria mentioned above.

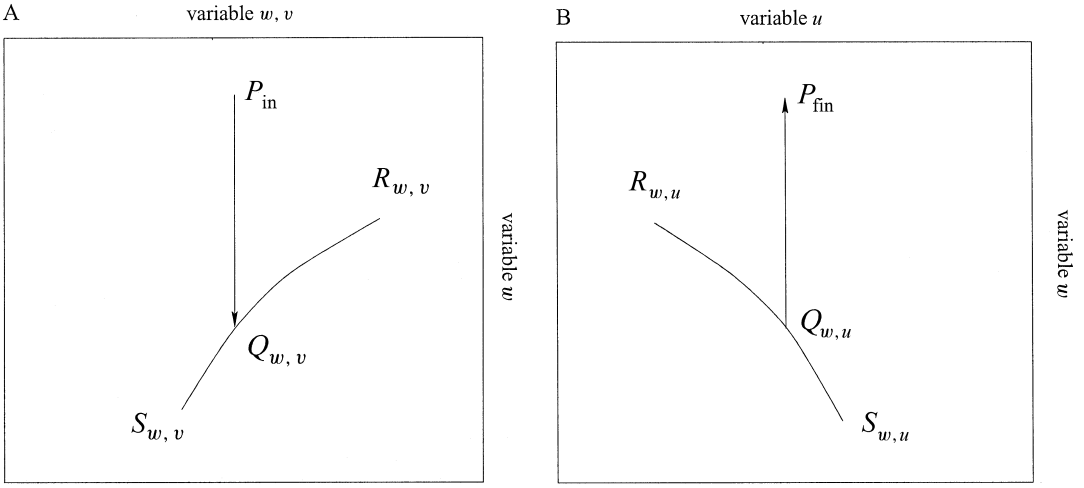

Figure 1. The possible slow curves and trajectories. Symbols designate: *a* – the slow curve $R_{wv}S_{wv}$ and the fast part $\Pi_{\text{in}}Q_{wv}$ of the trajectory in the plane v, w: *b* – the slow curve $R_{wu}S_{wu}$ and the fast part $Q_{wu}P_{\text{fin}}$ of the trajectory in the plane u, w; *c* – presentation of various trajectories in the plane θ, Π: $\Omega_{\text{i}}(R_iS_i)$ $(i = 1,2,3)$ – possible locations of the slow curve (due to various values of the flame velocities λ_F), $P_{\text{in}}Q_1P_1$, $P_{\text{in}}Q_2P_{\text{fin}}$, $P_{\text{in}}Q_3P_3$ – possible trajectories, $P_{\text{in}}Q_2P_{\text{fin}}$ – the single trajectory approaching the final point P_{fin}.

3.3.1. *A preheat subzone*

The variables v, w are the most suitable ones for analyzing the dynamics in the preheat subzone. Here w is a fast variable and v is a slow variable. For these variables the system (10–11) can be rewritten as follows:

$$\frac{\mathrm{d}w}{\mathrm{d}\xi} = H_R(\theta(w, v), \Pi(w, v)) - H_F(\theta(w, v), \Pi(w, v)), \tag{28}$$

$$\frac{\mathrm{d}v}{\mathrm{d}\xi} = H_R(\theta(w, v), \Pi(w, v)). \tag{29}$$

The slow curve of the singularly perturbed system is derived by equating the RHS of Equation (28) for the fast variable (w) to zero. Hence, for the preheat subzone, when v is the slow variable, the slow curve for the current system is given by the equation

$$\Omega_{wv} = H_R(\theta(w, v), \Pi(w, v)) - H_F(\theta(w, v), \Pi(w, v)) = 0. \tag{30}$$

It is good to underline here that the exact form and location of the slow curve depend on the value λ_F of the flame velocity, which serves as an unknown parameter of the problem (to be determined).

As we have already mentioned above, the slow surface may consist of stable and unstable parts, in the sense that they attract or repel trajectories. For the initial point P_{in}, the branch $R_{wv}S_{wv}$ of the slow curve Ω_{wv} is an attractor and the trajectory $P_{\text{in}}Q_{wv}$ moves towards it (Figure 1a). The trajectory moves in such a way that the value of the slow variable v conserves its initial value, while the value of the fast variable w changes rapidly. We can readily show that this initial stage of the system dynamics is characterized by a constant value of the concentration η, which conserves its initial value $\eta_0 = 1$. This outcome justifies our assumption that this part of the trajectory can be interpreted as the preheat subzone of the flame, where the temperature and pressure change only, while the concentration remains constant.

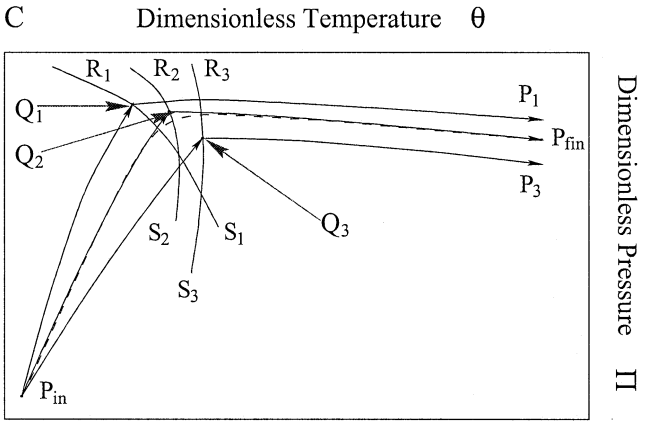

Figure 1. (Continued.)

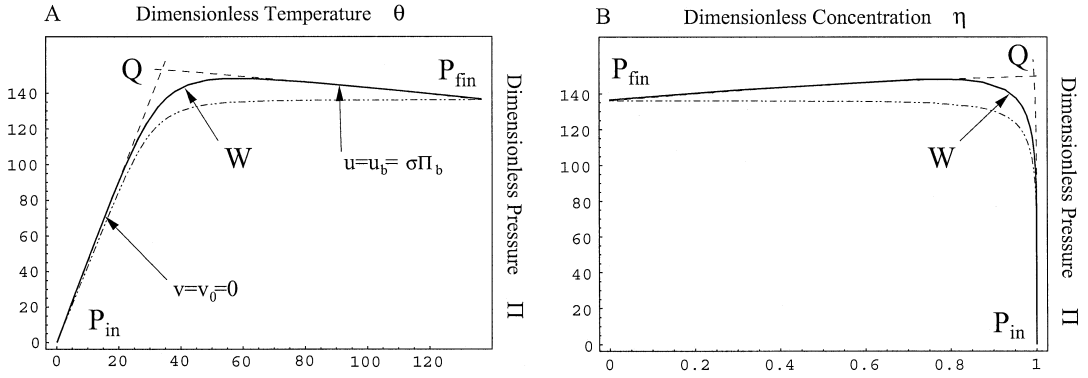

Figure 2. Projection of the systems; real trajectory on the planes θ, Π (a) and θ,η (b). Solid line $P_{\text{in}}WP_{\text{fin}}$ – result of numeric simulations of the considered model, chain-dashed line – result of numeric simulations of non-inertial model, dashed lines $P_{\text{in}}Q_2$ (preheat zone) and Q_2P_{fin} (reaction zone) – our approximations. The system parameters are $\beta = 0{\cdot}0295$; $\gamma = 1{\cdot}3$; $\varepsilon_1 = 6{\cdot}43 \times 10^{-6}$; $\varepsilon_2 = 4{\cdot}35 \times 10^{-8}$; $\sigma = 0{\cdot}23$; $q = 5{\cdot}66667$. The dimensionless flame velocity (used for dashed trajectory, numerical data) is $\lambda_F = 1{\cdot}42$ the dimensional one is $D = 72{\cdot}1$ m/s.

3.3.2. *B. Reaction subzone*

The variables u, w are the most suitable ones for analyzing the dynamics in the reaction subzone. Here w is a fast variable and u is slow. For these variables the system (10–11) can be rewritten as follows:

$$\frac{\mathrm{d}w}{\mathrm{d}\xi} = H_R(\theta(w,u),\ \Pi(w,u)) - H_F(\theta(w,u),\Pi(w,u)), \tag{31}$$

$$\frac{\mathrm{d}u}{\mathrm{d}\xi} = H_F(\theta(w,u),\ \Pi(w,u)). \tag{32}$$

The slow curve of the set of equations (singularly perturbed system) is derived by equating the RHS of Equation (28) for the fast variable (w) to zero. The slow curve for this zone *coincides* with the slow curve for the preheat zone:

$$\Omega_{wu}H_R(\theta(w,u),\Pi(w,u)) - H_F(\theta(w,v),\Pi(w,u)) = 0. \tag{33}$$

Just as the preheat subzone is handled we may analyze the reaction zone. For the initial point Q of this part of the trajectory the branch $R_{wu}S_{wu}$ of the slow curve Ω_{wu} (33) is repulsive and the trajectory $Q_{wu}P_{\text{fin}}$ moves from it in the direction of the final point P_{fin} that corresponds to the burnt mixture (Π_b, θ_b) (Figure 1b). Using (19), we can observe that the value of the slow variable u is constant and equal to its initial value. As in the previous stage, the value of the fast variable w changes fast.

3.3.3. *Entire trajectory*

One can easily see that the *same* equation of the slow curves (30) and (33) *de facto* represents the *same curve* for two different systems of coordinates: Ω_{wv} – in the (w, v) plane, Ω_{wu} – in the (w, u) plane. Hence, the points Q_{wu} (Figure 1a) and Q_{wv} (Figure 1b) should represent the *same* point Q in the original (Π, θ) plane. In other words, the final point Q_{wu} of the first part $P_{\text{in}}\ Q_{wu}$ (Figure 1a) of the trajectory should serve as the initial point Q_{wu} for the second part $Q_{wv}P_{\text{fin}}$ (Figure 1b) of the trajectory (the points Q_{wu} and Q_{wv} coincide with the point Q, Figure 1c).

Summarizing the previous analysis and combining the two dynamical scenarios described above, we can present an approximation of the entire trajectory of the system in the Π, θ plane in the following way (Figure 1c). Starting from the initial point P_{in}, the approximate trajectory $P_{\text{in}}Q_i$ $(i = 1, 2, 3)$ of the system moves toward the attracting branch R_iS_i $(i = 1, 2, 3)$. This part of the approximate trajectory matches to the part of the approximated trajectory presented in Figure 1a (preheat subzone) and it is characterized by a constant value of the system energy (the variable v is asymptotically constant in the (w, v) plane).

It would be worthwhile to recall here that the value of the flame velocity λ_F affects the following: location of the slow curve, the position of the matching point Q, the division of the phase plane into subzones and the choice of the coordinate systems in subzones. In Figure 1c we present positions of the slow curve, the matching point and the approximate trajectory for three different values of the flame velocity λ_F. The existence of a number of slow curves R_iS_i $(i = 1, 2, 3)$ and matching points Q_i $(i = 1, 2, 3)$ reflects this fact (different values of the index i correspond to different values of the flame velocity).

Only for a special value of the flame velocity λ_F the trajectory can reach the singular (final) point P_{fin} with coordinates $\Pi_{\text{b}} = \theta_{\text{b}} = \varepsilon_1/\varepsilon_2\gamma$. In Figure 1c this trajectory is depicted as $P_{\text{in}}Q_2P_{\text{in}}$ $(i = 2)$. This special trajectory contains the two parts. The first part has a starting point P_{in}. Once it is approaching the point Q_2, the trajectory changes its behavior. The part of the trajectory, starting at this point, moves in such a way that it approaches the singular (final) point P_{fin}. All other trajectories (such as $P_{\text{in}}Q_1P_1$ or $P_{\text{in}}Q_3P_3$) move above or below the final point P_{in}. This situation is illustrated in Figure 1c by $P_{\text{in}}Q_1P_1$ or $P_{\text{in}}Q_3P_3$. It would make sense to say that the part Q_2P_{fin} of the second trajectory $P_{\text{in}}Q_2P_{\text{fin}}$ is compatible with the trajectory $Q_{wu}P_{\text{fin}}$ presented in Figure 1b (reaction subzone) in the (w, u) plane. Its distinguishing feature is an approximate conservation law of the system's momentum (geometrically it means that the variable u is a slow variable in the (w, u) plane).

3.4. MATCHING POINT

Note, that the location of the final point P_{fin} does not depend on the flame velocity λ_F and has a permanent position in the phase plane. Therefore, the only way to find the desired trajectory ($P_{\text{in}}Q_2P_{\text{fin}}$; Figure 1c) is to vary the slow curve in such a way, that the matching point Q_2 belongs to it. To determine the location of the slow curve, we should match the two

different parts of the desired trajectory $P_{\text{in}}Q_2P_{\text{fin}}$ and to determine first the location of point Q_2. Actually, the point Q_2 serves as a matching point between the two parts of the approximate trajectory that corresponds to the preheat and reaction subzones of the flame front. Performing the matching, we remember that at the point Q_2 the variable u has the same value that it had in the starting point P_{in} of the trajectory $P_{\text{in}}Q_{wu}$ (Figure 1a). Similar to the variable u, the variable v at the point Q_2 has the same value that it had at the singular (final) point P_{fin} of the trajectory. Hence, we have the following system of equations for the evaluation of the coordinates of the point Q_2

$$\begin{aligned} &H_R(\theta_Q, \Pi_Q) - H_F(\theta_Q, \Pi_Q) = 0, \\ &u_Q = u_0 = 0; \quad v_Q = v_{\text{fin}} = v_b = \sigma\Pi_{\text{b}}, \end{aligned} \tag{34}$$

where θ_Q and Π_Q are the coordinates of point Q_2 in the Π, θ plane.

Remember that the first of these three equations (34) guarantees that the point Q_2 belongs to the slow curve and the last two are obtained from the asymptotic analysis of the system trajectory. The last two equations of (34) can be re-written in the form

$$\begin{cases} v_Q = v_{\text{fin}} = \sigma\Pi_{\text{b}} \\ u_Q = u_0 = 0 \end{cases} \Rightarrow \begin{cases} \sigma(\Pi_Q - \Pi_b) - \varepsilon_{\text{inert}}\dfrac{(\Pi_Q - \theta_Q)}{(1+\beta\Pi_Q)} = 0, \\ \theta_Q - \sigma\Pi_Q + \dfrac{1}{2}\varepsilon_{\text{inert}}\dfrac{(\Pi_Q - \theta_Q)^2}{(1+\beta\Pi_Q)^2} = 0. \end{cases} \tag{35}$$

The system (35) can be solved analytically as has already been done for a simpler case, when the impact of inertia was neglected [18]. In the model, the unknown values θ_Q and Π_Q represent explicit functions of the parameter $\varepsilon_{\text{inert}}$, describing the impact of the inertia phenomenon. We do not present here these functions, because we intend to use further an asymptotic expansion of $\theta_Q(\varepsilon_{\text{iner}})$ and $\Pi_Q(\varepsilon_{\text{inert}})$ as functions of the small parameter $\varepsilon_{\text{inert}}$.

3.5. Flame velocity

An analytical expression for the flame velocity λ_F can be determined in the following manner. During the first stage we consider the functions $\theta_Q(\varepsilon_{\text{inert}})$ and $\Pi_Q(\varepsilon_{\text{inert}})$ as they are determined by the system (35). In the second step we derive a relation between the flame velocity λ_F and the inertia parameter $\varepsilon_{\text{inert}}$. Finally, we substitute all these relations as functions of the inertia parameter $\varepsilon_{\text{inert}}$ in the first of the three relations (34). Recall that this equation means that the matching point Q_2 belongs to the slow curve Ω.

The equation that is finally obtained,

$$\lambda_{\text{F}}^3\left(\varepsilon_{\text{inert}}\right)\left(\Pi_Q(\varepsilon_{\text{inert}}) - \theta_Q(\varepsilon_{\text{inert}})\right)^2 - \varepsilon_1\left(1+\beta\Pi_Q(\varepsilon_{\text{inert}})\right)^2 \exp\left(\frac{\theta_Q(\varepsilon_{\text{inert}})}{1+\beta\theta_Q(\varepsilon_{\text{inert}})}\right) = 0 \tag{36}$$

with respect to the unknown inertia parameter $\varepsilon_{\text{inert}}$, allows us to determine its value, and, using a connection between $\varepsilon_{\text{inert}}$ and λ_F, to get finally an approximate formula for the flame velocity λ_F.

Let us return to the functions $\theta_Q(\varepsilon_{\text{inert}})$ and $\Pi_Q(\varepsilon_{\text{inert}})$, which were derived as a solution of the system (35). Owing to the region of the flame velocities considered here (subsonic flames), the value of the parameter $\varepsilon_{\text{inert}}$, responsible for the inertia phenomenon, is relatively small (with respect to unity). Therefore, the functions ($\theta_Q(\varepsilon_{\text{inert}})$ and $\Pi_Q(\varepsilon_{\text{inert}})$ can be expanded

with respect to the small parameter $\varepsilon_{\text{inert}}$. For our purpose an expansion of the first order is sufficient. It reads

$$\Pi_Q = A_0 + \varepsilon_{\text{inert}} A_1, \quad \theta_Q = B_0 + \varepsilon_{\text{inert}} B_1, \tag{37}$$

where the coefficient A_0, A_1, B_0, B_1 are defined as follows:

$$\begin{aligned} A_0 &= \Pi_{\text{b}},\ A_1 = \frac{\Pi_{\text{b}}(1-\sigma)}{\sigma\beta(1+\beta\Pi_{\text{b}})},\ C = \frac{K_{\text{F}}}{A}\left(\frac{C_{\text{p}}T_0}{\beta}\exp\left(\frac{1}{\beta}\right)\right)^{1/2}, \\ B_0 &= \sigma\Pi_{\text{b}},\ B_1 = \left(\frac{\Pi_{\text{b}}(1-\sigma)}{\beta(1+\beta\Pi_{\text{b}})} - \frac{1}{2}\frac{\Pi_{\text{b}}^2(1-\sigma)^2}{(1+\beta\Pi_{\text{b}})^2}\right). \end{aligned} \tag{38}$$

At the current stage of the analysis let us draw the attention of the reader to the definition (14) of the inertia parameter $\varepsilon_{\text{inert}}$ and expression (15) of the dimensionless flame velocity λ_F via its dimensional counterpart. The parameter $\varepsilon_{\text{inert}}$ is proportional to the square of the dimensional flame velocity D (14), whereas the dimensionless flame velocity λ_F is directly proportional to the dimensional flame velocity D (15). Hence, within the framework of the accepted model, there is a simple connection between the expression λ_F^3 and the inertia parameter $\varepsilon_{\text{inert}}$: $\lambda_F^3 = C\varepsilon_{\text{inert}}^{3/2}$.

This relation and the expansions (37) can be substituted in Equation (34) (the slow-curve equation). After simplification, Equation (36) can be rewritten as

$$D_0 + \varepsilon_{\text{inert}} D_1 + \varepsilon_{\text{inert}}^{3/2} D_{3/2} + \varepsilon_{\text{inert}}^{5/2} D_{5/2} = 0, \tag{39}$$

where the coefficients D_0, D_1, $D_{3/2}$, $D_{5/2}$ are given as follows:

$$\begin{aligned} D_0 &= -\varepsilon_1(1+\beta A_0)^2 \exp\left(\frac{B_0}{1+\beta B_0}\right), \\ D_1 &= -\varepsilon_1(1+\beta A_0)\exp\left(\frac{B_0}{1+\beta B_0}\right)\left(2\beta A_1 + \frac{(1+\beta A_0)}{(1+\beta B_0)^2}B_1\right), \\ D_{3/2} &= (A_0 - B_0)^2 C;\ D_{5/2} = 2(A_0 - B_0)(A_1 - B_1)C. \end{aligned} \tag{40}$$

Equation (39) is an equation for the inertia parameter $\varepsilon_{\text{inert}}$ and can be solved numerically. Exploiting definition (14) of the parameter $\varepsilon_{\text{inert}}$ responsible for the inertia impact, one can get a relation between $\varepsilon_{\text{inert}}$ and the dimensional flame velocity D

$$\varepsilon_{\text{inert}} = \frac{\beta D^2}{C_{\text{p}}T_0} \Rightarrow D^2 = c_{\text{p}}T_0\frac{\varepsilon_{\text{inert}}}{\beta} = \frac{\varepsilon_{\text{inert}}}{(\gamma-1)\beta}. \tag{41}$$

4. Discussion

The equation (coordinates) allows us to estimate the impact of the inertia phenomenon on the flame velocity. Preliminary estimates show that, within the chosen region of the flame velocities (subsonic flames), the correction to the flame speed due to inertia should be of order of the small parameter β. Indeed, expression (14) for the parameter $\varepsilon_{\text{inert}}$ can be rewritten in the form

$$\varepsilon_{\text{inert}} = \frac{\beta D^2}{c_{\text{p}}T_0} = (\gamma-1)\beta\frac{D^2}{a_0^2} = (\gamma-1)\beta M^2, \tag{42}$$

where a_0 is the sound velocity in the fresh mixture, M is the Mach number computed with respect to the velocity of sound in the fresh mixture. Under the accepted assumption regarding the subsonic character of the flame ($M < 1$), the value of the parameter $\varepsilon_{\text{inert}}$ remains of the order of the small parameter β. The physics lying behind this conclusion is rather simple: within the chosen region of the flame velocities, the impact of the inertia phenomenon is small with respect to the governing mechanisms (pressure diffusion and chemical reaction).

4.1. Consistence with the previous results

Neglecting the inertia phenomenon should provide us with the result obtained earlier for a pressure-driven flame in a porous medium [18]. To perform this transformation correctly, we have to neglect the impact of the inertia phenomenon (to equate the inertia parameter $\varepsilon_{\text{inert}}$ to zero in the Equations (18), (19)). The expressions for the variables u, v. are sufficiently simplified and read

$$u = \sigma\Pi; \quad v = \theta - \sigma\Pi \tag{43}$$

Adopting the approach described above, we can easily determine the coordinates of the matching point Q_2 dividing the flame front into preheat and reaction subzones. The desired coordinates are as follows

$$\theta_Q = \sigma\Pi_{\text{b}}, \quad \Pi_{\text{Q}} = \Pi_{\text{b}} = \frac{\varepsilon_1\gamma}{\varepsilon_2}, \quad \eta_Q = 1. \tag{44}$$

Once we have obtained these values, we will be able to derive an analytical expression for the flame velocity λ_F using Equation (34) for the slow curve. The formula for the flame velocity in the non-inertial case can be written as

$$\lambda_{\text{F}}^3 = \frac{\varepsilon_1(1+\beta\Pi_{\text{Q}})^2 \exp\left(\frac{\theta_{\text{Q}}}{1+\beta\theta_{\text{Q}}}\right)}{(\Pi_{\text{Q}} - \theta_{\text{Q}})^2}. \tag{45}$$

Expression (45) coincides with the expression that was derived earlier by the authors for a model without inertia effects [18]. One can see that structure of the expression (45) resembles the well-known formula for the flame speed for gaseous combustion as suggested in [17, Chapter 4], where the flame velocity is proportional to the square root of the Arrhenius exponent. Unlike Zel'dovich's formula [17, Chapter 4], expression (45) provides us with an unusual dependence of the flame velocity on the Arrhenius exponent, namely a cubic-root dependence of the Arrhenius exponent, where the power of the exponent is determined by the temperature at the point Q_2 serving as a boundary between the two subzones of the flame.

There is good reason to note here that our prediction (45) for the flame velocity in the case of zero impact of inertia coincides with results [11] (for a particular case) that were obtained on the basis of the rather cumbersome modification of the conventional multi-scale approach. This fact lends credit to the approach suggested in the present paper.

4.2. Prediction *vs* numerics

To check the correctness of the theoretical formulae, a number of direct numerical simulations have been performed. The Cauchy problem for the system of dimensionless equations (10–12) has been solved numerically for some typical combinations of the parameter values. Here we present a comparative analysis of the theoretical predictions and the numerical simulations.

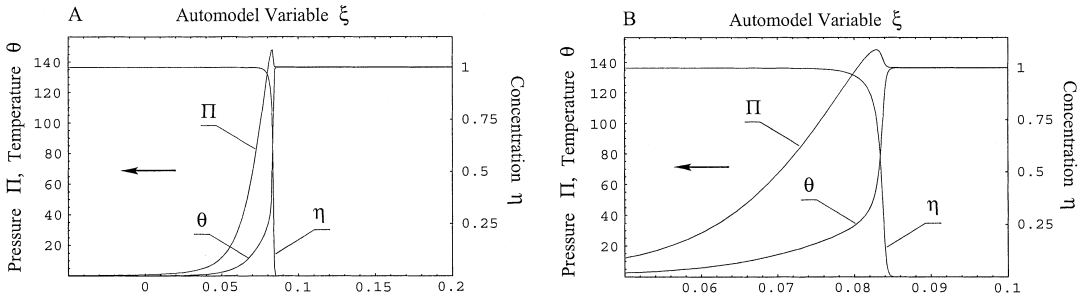

Figure 3. Typical time histories of the flame front of the considered problem. For the system parameters see caption of Figure 2.

Figure 2 allows us to get a visual impression of how the approximation based on the asymptotic approach (MIM) describes a real trajectory in phase space. The figure is a projection of the real trajectory in the three-dimensional space Π, θ, η onto the (θ, Π) plane (Figure 2a) and the (θ, η) plane (Figure 2b). The smooth solid curve $P_{\text{in}}WP_{\text{fin}}$ represents the result of a direct numerical simulation, whereas the dashed lines $P_{\text{in}}Q_2$ and Q_2P_{fin} are based *on* the asymptotic approximations (MIM, within preheat and reaction subzones). The approximation $P_{\text{in}}Q_2$ of the preheat sub-zone corresponds to the stage $P_{\text{in}}Q_{wv}$ (Figure 1a) and to the component $P_{\text{in}}Q_2$ in Figure 1c. In turn, the approximation Q_2P_{fin} of the reaction subzone relates to the component $Q_{wu}P_{\text{fin}}$ (Figure 1b) and section Q_2P_{fin} in Figure 1c.

One can see that, within the preheat subzone (θ in the interval 0–50), the energy of the system is almost constant; a difference between the two curves (theoretical and numerical) is not visible. Visually the pressure Π is strictly proportional to the temperature θ. A cause of this proportionality can be found in expression (18). As we have already mentioned above, within the accepted region of flame velocities, the parameter $\varepsilon_{\text{inert}}$ is small, and relation (18) reads as $v = \sigma\Pi - \theta$. Taking into account the fact that the variable v is slow within the preheat subzone (asymptotically the variable v conserves its initial zero value within the chosen subzone), one can easily understand the proportionality $\Pi \sim \theta$. The coefficient of proportionality (σ) is larger than unity, which means that the pressure rises faster than the temperature. A beginning discrepancy is observable only in the vicinity of the point Q_2 (a matching point dividing the flame front into two subzones), where the character of the trajectory changes.

In a similar way one can ensure that the momentum of the system conserves its final value within the reaction subzone with rather good accuracy. It is difficult to distinguish two curves (solid and dashed ones) within the interval [70, 200] of θ-values. This testifies to the fact that the suggestion made regarding the approximate nature of the law of momentum conservation was fairly reasonable. One can see that the approximation looks reasonable and the most discrepancy is observed in the neighborhood of point Q_2.

The computed results for the temperature, pressure and fuel concentration are presented in Figure 3 and should be considered together with the analytical predictions of the Figures 1a and 1b. In Figure 3 one can see that the pressure Π and the temperature θ begin to change in the preheat subzone (the pressure Π rises faster than the temperature (θ), while the value of the concentration η appears to be constant (the energy of the system – the variable v is asymptotically constant). The pressure rises and at some point reaches a value higher than its final value. Just after that, the temperature θ and the concentration η start alternating rather fast, while the pressure Π appears to be constant (momentum of the system – the variable

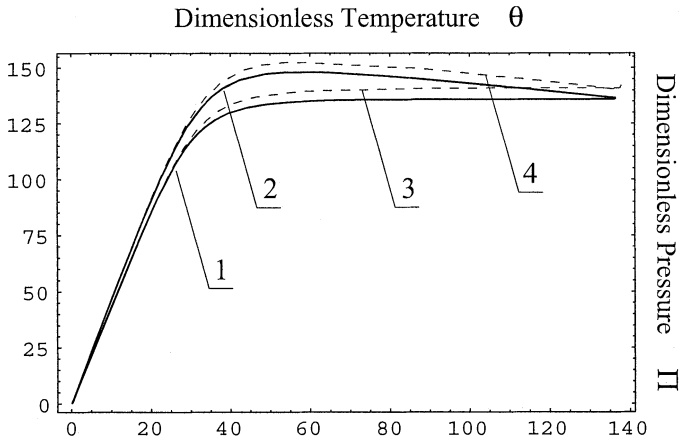

Figure 4. Typical structure of the flame front of the considered problem. For the system parameters see caption to Figure 2.

u – is asymptotically constant within this subzone). One can see that, in accordance with the theoretical predictions made earlier, the pressure rises more quickly than the temperature and reaches its final value (pressure of the reaction products) at the point located very closely to the point where the temperature jumps. This is the point Q_2 separating the two subzones of the flame (reaction and preheat).

Figure 4 illustrates how the pressure Π changes as the dimensionless temperature θ increases for two different cases, namely with and without inertia effects. The solid curves 1 and 2 depict results of a numerical solution of the original system. The simulations make the difference in the flame structure apparent – line 2 (inertia ON) has a maximum in the vicinity of $\theta \sim 50$, whereas line 1 (inertia OFF) approaches its final maximum value. One can also see that, just after the maximum point, curve 2 smoothly decreases to its final adiabatic value, while line 1 remains constant. Curves 3 (inertia OFF) and 4 (inertia ON) present our analytic approximations. One can conclude that the accuracy of the approximations is fairly good and the applied asymptotic approach slightly overestimates the function $\Pi(\theta)$.

It would make sense to note here that an arbitrary asymptotic tool is able to provide us with results that are *asymptotically* correct (general case). Nevertheless, as we will see further in the problem under consideration, the discrepancy between the analytical formulae and the results of the numerical simulations are quite good. This lends credit to the suggested asymptotic method.

The dependence of the dimensional flame velocity D on the small parameter β for different cases and the accuracy of the theoretical predictions are presented in Figure 5. As in the previous figure, the solid curves in Figure 5a depict numerical results, whereas the dashed lines are the theoretical predictions. The odd numbers correspond to the non-inertial case, whilst the even numbers (2, 4) relate to the model with inertia taken into account and compares theoretical predictions (45) (estimates of the flame velocity λ_F) and numerical data. The speed of the flame grows when the parameter β is increased.

The accuracy of the analytical prediction can be estimated by the formula

$$\left(\frac{\lambda_F^{\text{theor}} - \lambda_F^{\text{num}}}{\lambda_F^{\text{num}}} 100\right) (\%), \tag{46}$$

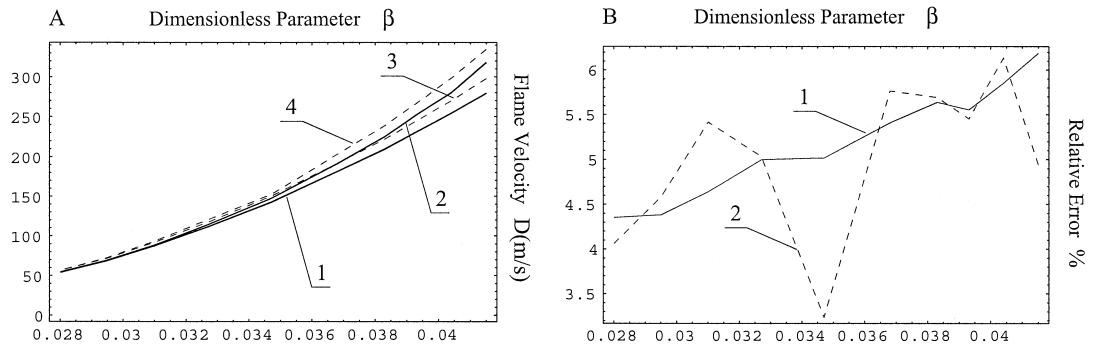

Figure 5. Theoretical predictions (41) and (45) of the flame-velocity dependence on the dimensionless parameter β *vs* results of numerical simulations. a. Dimensional flame velocity D *vs.* parameter β. Solid lines – numerical simulations, dashed ones – theoretical predictions; the odd numbers (1,3) – non-inertial model; the even numbers (2,4) – inertia accounted for. b. Relative accuracy (46) of the theoretical formulae (41) and (45) *vs.* the dimensionless parameter β. Digits designate: 1 – relative accuracy of the approximation (45) compared with numerics for the non-inertial model (relative difference between the lines 1 and 3 in Figure 5a); 2 – relative accuracy of the approximation (41) compared with numerics for inertial model (relative difference between the lines 2 and 4 in Figure 5a). c. Relative accuracy (46) of the theoretical formulae (41) and (45) *vs.* the dimensionless parameter β. Digits designate: 1 – relative accuracy of the approximation (41) compared with numerics for the full model (relative difference between the lines 2 and 4 in Figure 5a); 2 – relative accuracy of the approximation (45) compared with numerics for the full model (relative difference between the lines 2 and 3 in Figure 5a).

where λ_F^{theor} is the theoretical prediction (45) for the flame velocity and λ_F^{num} represents results of an appropriate numerical simulation. In Figure 5b the results of the comparison are plotted. Curve 1 presents the relative accuracy of our approximation for the non-inertial model (relative difference between the lines 1 and 3 in Figure 5a), whereas line 2 depicts the result of an application of Equation (46) to the model with the inertia mechanism accounted for. Figure 5c illustrates how the accuracy of the asymptotic formulae (41) and (45) changes as the parameter β increases. Both calculations were performed with respect to a numerical simulation of the model with inertia accounted for. In fact, curve 1 in Figure 5c presents the relative difference between the lines 2 and 4 in the Figure 5a (relative error is and remains positive), whereas the bends 2 in Figure 5c depict a relation benveen the curves 2 and 3 (relative error quickly becomes and remains negative). The analysis of the relevant numerical simulations shows that the accuracy of the theoretical predictions sufficiently depends on the chosen parametric region. For the specific set of the problem parameters, the relative error of the analytical formulae is about 4–6% and grows (an absolute value) slowly within this interval as the parameter β increases.

Figure 6 demonstrates how the dimensional flame velocity D changes as the coefficient of the quadratic friction force K_F increases. Figure 6 compares the theoretical predictions (41) and (45) and numerical data resulting from numerical simulations. The flame speed increases sharply in the region of small values of β and tends to some constant value when β increases. The accuracy (46) of the explicit expression (45) in the parametric region used for the simulations presented in the figures is about 3–7%. Note here that the absolute error of the prediction (the absolute value of the difference between the theoretical and the numerical results) seems almost constant and does not demonstrate any visible dependence on β.

The discrepancy between the analytical formula obtained by the MIM and the results of the numerical simulations can be regarded as fairly good.

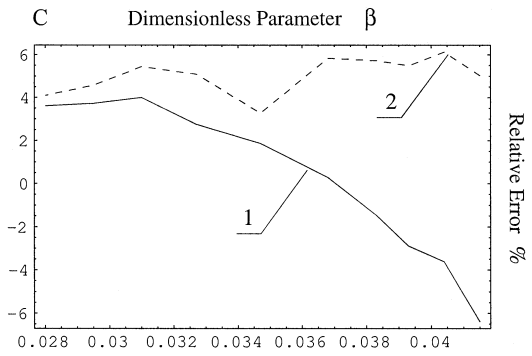

Figure 5. (Continued.)

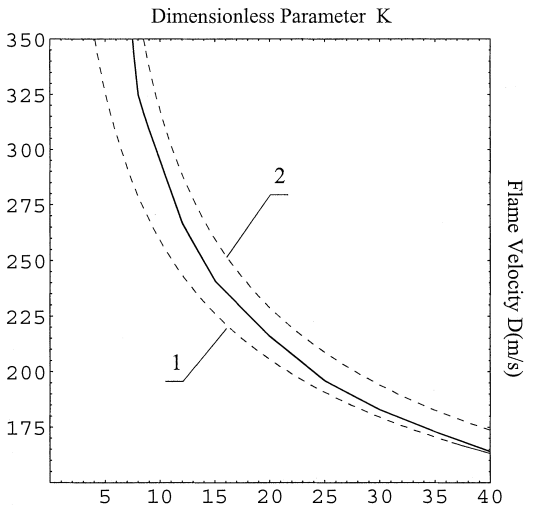

Figure 6. Dimensional flame velocity D *vs.* friction parameter K_F. The solid line represents the results of direct numerical simulations. Digits designate (dashed lines): 1 – non-inertial theoretical prediction (45), 2 – analytical estimate (41) (inertia phenomenon is accounted for).

5. Conclusions

It is now a well-established experimental fact that flames spreading through an inert porous medium filled with combustible gas may have unusual properties [1]. One of the main reasons for these phenomena is the crucial role of the hydrodynamic conditions of the gas flow through a porous medium for the determination of the flame properties. The present paper has been devoted to the asymptotic study of the inertia effect on the behavior of a pressure-driven flame in a porous medium. The suggested asymptotic approach permitted – for the first time – to obtain an analytical asymptotic solution of the problem under consideration.

To recapitulate the analysis of the inertia effect on the structure of a pressure-driven flame in a porous medium, let us summarize the main ideas and results of our study. The specific problem of flame propagation in a porous medium, where a driving force is the local elevation of the pressure, rather than the conventional mechanism of heat diffusion, was considered and analyzed. The physical model of the phenomenon incorporated the exothermic chemical reaction, the diffusion of the gas pressure, the friction force, and the inertia of the moving fluid. The mathematical model of the phenomenon originally involved five nonlinear partial differential equations. The system was reduced to a system of ordinary differential equations in the frame of coordinates related to the propagating combustion wave. The reduced system represents a singularly perturbed system of ODEs and was studied using a new heuristic approach for the analysis of the flame-propagation problem (a modified version of the MIM – method of integral manifolds).

The analysis of the system trajectory in the phase space allowed us to conclude that the trajectory consists of two stages having rather distinct properties. The first stage is characterized by an approximate law of energy conservation and represents the fast motion from the initial point in the direction of the attractive branch of the slow curve. While the fast motion takes

place, the slow variable (introduced on the basis of the system-energy expression) conserves its initial value. The second stage is distinguished by an approximate law of momentum conservation. During the second stage, a fast motion occurs from the repulsive branch of the manifold to the final stationary point. The slow variable (based on the momentum of the system) conserves the value obtained at the matching point Q. These two subsequent stages of the trajectory correspond to the two obvious physical subzones of the flame front. The first stage can be associated with the preheat subzone of the flame, whereas the second can be interpreted as the reaction subzone. Therefore, the flame front can be conditionally subdivided into two subzones, namely the preheat and the reaction subzones. The matching point Q separating these two subzones plays a key role in the determination of the flame velocity.

The suggested approach allowed us to get an analytical estimate of the inertia effect on the flame velocity. The desired estimate represents a solution of the algebraic equation (39). We have shown, that, in the absence of the inertia, the flame velocity is proportional to the cubic root of the Arrhenius exponent (45), which coincides with our earlier results [18]. The impact of inertia grows with increasing flame velocity. The inertia influence becomes significant (up to 15%) in the parametric region, where the speed of the combustion wave approaches the sound velocity in a fresh mixture (for Mach number close to unity). The theoretical predictions demonstrated good agreement with direct numerical simulations.

Finally, we note that, although the presented application of the modified MIM approach to the model for pressure-driven flames in porous media does provide a broader more accurate perspective than that previously obtained with non-inertial models, it is not devoid of deficiencies. It is indisputable that a more realistic description should ideally include one or more additional effects: the wider region of the flame velocities (inertia impact is expected to be larger), thermal diffusion (conventional mechanism of flame propagation), more details of the chemistry such that initiation of the chemistry via a radical pool can be accounted for, etc. These directions for further improvement of our model are currently under investigation.

Acknowledgements

Authors are most grateful to Gregory Sivashinsky and Peter Gordon for fruitful discussions. Igor Goldfarb is grateful to the German-Israeli Foundation (Grant G-695-15.10/2001) for financial support.

References

1. V.S. Babkin, Filtration combustion of gases. present state of affairs and prospects. *Pure Appl. Chemistry* 64 (1993) 335–344.
2. V. Gol'dshtein, I. Shreiber and G. Sivashinsky, On creeping detonation in filtration combustion. *Shock Waves* 4 (1994) 109–112.
3. I. Brailovsky, V. Gol'dshtein, I. Shreiber and G. Sivashinsky, On combustion wave driven by diffusion of pressure. *Combust. Sci. Technol.* 124 (1997) 145–165.
4. I. Brailovsky, M. Frankel and G. Sivashinsky, Galloping and spinning modes of subsonic detonation. *Combust. Theory Modell.* 4 (2000) 47–60.
5. Yu. A. Mitropolskiy and O.B. Lykova, *Lectures on the Methods of Integral Manifolds*, (in Russian). Kiev: Institute of Mathematics, Ukrainen Akademy of Science, (1968) 416 pp.
6. N.N. Bogolyubov and Yu. A. Mitropolsky, *Asymptotic Methods in the Theory of Nonlinear Oscillations*. N. Y. Gordon and Breach (1961) 537 pp.

7. V. Sobolev and V. Strygin, *Decomposition of Motions by the Integral Manifolds Method*. Moscow: Nauka (in Russian) (1988) 256 pp.
8. V.M. Gol'dshtein and V. Sobolev, Integral manifolds in chemical kinetics and combustion, *American Mathematical Society Translations*, Series 2, 153 (1992) pp. 73–92.
9. I. Brailovsky and G. Sivashinsky, Hydraulic resistance as a mechanism for deflagration-to-detonation transition. *Combust. Flame* 122 (2000) 492–499.
10. I. Goldfarb, V. Gol'dshtein and G. Kuzmenko, Pressure driven flame in porous media. *Phys. Lett. A* 251 (1999) 394–403.
11. P.V. Gordon and G.I. Sivashinsky (2001) Private conversation.
12. N.N. Semenov, Zur Theorie des Verbrennungsprozesses. *Zeitschr. Phys.* 48 (1928) 571–581.
13. D.A. Frank-Kamenetskii, *Diffusion and Heat Exchange in Chemical Kinetics*, 2nd edn. New York: Plenum Press (1969) 574 pp.
14. N. Fenichel, Geometric singular perturbation theory for ordinary differential equations. *J. Diff. Equ.* 31 (1979) 53–98.
15. I. Goldfarb, V.Gol'dshtein, G. Kuzmenko and J.B. Greenberg, On thermal explosion of a cool spray in a hot gas. In: F. Dryer and T. Burgess (eds.), *Twenty-Seventh Symposium (International) on Combustion*. The Combustion Institute, Pittsburg, PA (1998) pp. 2367-2371.
16. I. Goldfarb, V. Gol'dshtein and A. Zinoviev, Delayed thermal explosion in porous media: method of integral manifolds. *IMA J. Appl. Math.* 67 (2002) 263–280.
17. Ya.B. Zel'dovich, G.I. Barenblatt, V.B. Librovich and G.M. Makhviladze, *Mathematical Theory of Combustion and Explosions*. New York: Plenum (1985) 597 pp.
18. V. Bykov, I. Goldfarb and V. Gol'dshtein, On the integral manifolds approach in a flame propagation problem: pressure driven flames in porous media. *IMA J. Appl. Math.* (2003) accepted for publication.